

RESEARCH ARTICLE

Intracellular glycine receptor function facilitates glioma formation *in vivo*

Benjamin Förster^{1,*}, Omar Dildar a Dzaye^{2,*}, Aline Winkelmann^{1,3}, Marcus Semtner¹, Bruno Benedetti⁴, Darko S. Markovic⁵, Michael Synowitz⁶, Peter Wend⁷, Michael Fähling⁸, Marie-Pierre Junier⁹, Rainer Glass¹⁰, Helmut Kettenmann² and Jochen C. Meier^{1,‡}

ABSTRACT

The neuronal function of Cys-loop neurotransmitter receptors is established; however, their role in non-neuronal cells is poorly defined. As brain tumors are enriched in the neurotransmitter glycine, we studied the expression and function of glycine receptors (GlyRs) in glioma cells. Human brain tumor biopsies selectively expressed the GlyR $\alpha 1$ and $\alpha 3$ subunits, which have nuclear localization signals (NLSs). The mouse glioma cell line GL261 expressed GlyR $\alpha 1$, and knockdown of GlyR $\alpha 1$ protein expression impaired the self-renewal capacity and tumorigenicity of GL261 glioma cells, as shown by a neurosphere assay and GL261 cell inoculation *in vivo*, respectively. We furthermore showed that the pronounced tumorigenic effect of GlyR $\alpha 1$ relies on a new intracellular signaling function that depends on the NLS region in the large cytosolic loop and impacts on GL261 glioma cell gene regulation. Stable expression of GlyR $\alpha 1$ and $\alpha 3$ loops rescued the self-renewal capacity of GlyR $\alpha 1$ knockdown cells, which demonstrates their functional equivalence. The new intracellular signaling function identified here goes beyond the well-established role of GlyRs as neuronal ligand-gated ion channels and defines NLS-containing GlyRs as new potential targets for brain tumor therapies.

KEY WORDS: Glycine receptor, Gene regulation, Glioma

INTRODUCTION

Glycine receptors (GlyRs) belong to the Cys-loop neurotransmitter receptor family of ligand-gated ion channels. Members of this receptor family have a similar protein architecture, with an extracellular ligand-binding domain, four transmembrane segments and a large cytosolic loop domain

between transmembrane segments 3 and 4. Four genes (*Gla1–Gla4*) coding for GlyR $\alpha 1–\alpha 4$ subunits have been identified, and each of these subunits is able to produce functional homomeric glycine-gated Cl^- channels (Harvey et al., 2000; Kuhse et al., 1991; Malosio et al., 1991; Nikolic et al., 1998). In humans, however, *GLRA4* is a pseudogene (Simon et al., 2004). A single gene (*Glyrb*) delivers cells with the GlyR β subunit, which mediates postsynaptic receptor anchoring (Meier et al., 2001; Meyer et al., 1995) and can contribute to glycine binding (Grudzinska et al., 2005), but is unable to produce functional homo-pentameric GlyR channels. GlyR $\alpha 1$ and $\alpha 3$ structurally differ from the $\alpha 2$, $\alpha 4$ or β subunits as they contain a functional nuclear localization signal (NLS) in the large cytosolic loop domain (Melzer et al., 2010). It has been established that the NLS interacts with nuclear import proteins of the karyopherin family (importin $\alpha 3$ and $\alpha 4$) (Melzer et al., 2010), but although the functional role of this sequence determinant has remained elusive, it has been suggested to play a role in non-neuronal cells (den Eynden et al., 2009). Brain tumors are enriched in the neurotransmitter glycine (Bobek-Billewicz et al., 2010), which raises the question as to whether glioma cell GlyRs serve a classical neurotransmitter receptor function or use their NLS for intracellular signaling.

Here, we addressed this question and discovered that the NLS-harboring GlyR $\alpha 1$ and $\alpha 3$ subunits were expressed in human brain tumor biopsies. We found that glioma cell GlyRs were retained in intracellular compartments and did not serve as neurotransmitter receptors. To study the functional role of intracellular GlyR expression in glioma cells, we used the mouse glioma cell line GL261, which specifically expresses the GlyR $\alpha 1$ RNA splice variant (Malosio et al., 1991) with hitherto unknown function. Knockdown of GlyR $\alpha 1$ protein expression impaired tumorigenicity and self-renewal capacity. The pronounced anti-tumor effect of reduced GlyR $\alpha 1$ protein expression relied on an intracellular GlyR signaling function that was mediated by the large cytosolic loop domain, including the GlyR-intrinsic NLS, which ultimately regulated the expression of tumor cell genes. The GlyR target genes included proto-oncogenes, molecules involved in signaling pathways downstream of extracellular-signal-regulated kinase (ERK) and β -catenin/Wnt, transcription factors, and a plethora of gene products that are known to be involved in determining self-renewal capacity ('stemness'). That the self-renewal capacity of GlyR $\alpha 1$ knockdown GL261 cells was rescued upon stable expression of the GlyR $\alpha 1$ and $\alpha 3$ loops furthermore demonstrates the functional equivalence of both GlyR subunits in brain tumor cells.

¹RNA editing and Hyperexcitability Disorders Helmholtz Group, Max Delbrück Center for Molecular Medicine, 13092 Berlin, Germany. ²Cellular Neuroscience, Max Delbrück Center for Molecular Medicine, 13092 Berlin, Germany. ³FU-Berlin, Fachbereich Biologie, Chemie, Pharmazie, Takustrasse 3, 14195 Berlin. ⁴Department for Physiology, Innsbruck Medical University, 6020 Innsbruck, Austria. ⁵Department for Neurosurgery, Helios Clinic Buch, 13125 Berlin, Germany. ⁶Department for Neurosurgery, Charité Universitätsmedizin Berlin, 13353 Berlin, Germany. ⁷David Geffen School of Medicine at UCLA, UCLA Jonsson Comprehensive Cancer Center, 10833 LeConte Avenue, CHS 27-139, Los Angeles, CA. 90095, USA. ⁸Institut für Vegetative Physiologie, Charité Universitätsmedizin Berlin, 10117 Berlin, Germany. ⁹INSERM U894, Psychiatry and Neuroscience Center, Glial Plasticity Team, Paris 75014, France. ¹⁰Neurosurgical Research, University Clinics Munich, 81377 München, Germany. *These authors contributed equally to this work

[‡]Author for correspondence (jochen.meier@mhc-berlin.de)

RESULTS

GlyR $\alpha 1$ and $\alpha 3$ are expressed in human brain tumors and stem cells

To study GlyR expression in human glioma biopsies, quantitative real-time PCR analysis of GlyR $\alpha 1$ -, $\alpha 2$ - and $\alpha 3$ -encoding mRNA was performed on a β -actin-normalized cDNA panel of pathologist-verified human brain tumors (supplementary material Table S1). We did not include the $\alpha 4$ subunit into our analyses because this type of GlyR will not form functional glycine-gated receptor channels at the cell surface due to a premature stop codon encoded in the human *GLRA4* gene (Simon et al., 2004). Following amplification of the samples, PCR products were analyzed with agarose gel electrophoresis, and a sample was only included into our quantitative expression analysis if a single band with the correct molecular mass was detected. *GLRA1* gene expression was detected primarily in World Health Organization (WHO) grade II and III tumors, whereas *GLRA3* gene expression was more widespread and found throughout WHO grade I–IV tumors (Fig. 1; supplementary material Table S1). GlyR $\alpha 2$ -encoding mRNA was not detected (except case number 36).

We next analyzed expression of GlyR $\alpha 1$ and $\alpha 3$ subunits in established and well-characterized human stem-cell-like glioma cells (Galan-Moya et al., 2011; Silvestre et al., 2011; Thirant et al., 2011) (supplementary material Table S2). mRNA coding for the GlyR $\alpha 1$ ins RNA splice variant (Malosio et al., 1991) was detected in three out of six stem-cell-like cell samples from adult oligoastrocytoma and glioblastoma multiforme (Galan-Moya et al., 2011; Silvestre et al., 2011), whereas GlyR $\alpha 1$ -encoding mRNA in stem-cell-like cells from pediatric glioma (Thirant et al., 2011) lacked the RNA splice insert (supplementary material Table S2). GlyR $\alpha 3$ -coding mRNA was detected in all the analyzed samples (supplementary material Table S2). Moreover, the vast majority (nine out of 11) of stem-cell-like cells expressed the GlyR $\alpha 3$ K RNA splice variant (Nikolic et al., 1998), which sets this cell type apart from neurons with regard to prevailing expression of the long GlyR $\alpha 3$ L RNA splice variant in neurons (Eichler et al., 2009).

Characteristics of GlyR expression in mouse GL261 glioma cells

We used here the EGFP-expressing mouse cell line GL261 (Walzlein et al., 2008), which is commonly used for the

generation of experimental brain tumors in mice. GL261 cells selectively express mRNA coding only for the GlyR $\alpha 1$ ins RNA splice variant (Malosio et al., 1991), and not for $\alpha 2$, $\alpha 3$, $\alpha 4$ or β subunits (Fig. 2A). To confirm that GlyR $\alpha 1$ ins-coding mRNA results in expression of receptor protein, we used a polyclonal GlyR $\alpha 1$ -directed antibody for immunochemical analysis of GL261 cells (Fig. 2B). Strong GlyR $\alpha 1$ protein expression was found in $10\% \pm 5$ (\pm s.d., $n=3$ experiments) of GL261 cells. We verified that polyclonal GlyR $\alpha 1$ antibody-dependent signals were specific as evidenced by the congruency of immunochemical signals generated in combination with the well-characterized GlyR $\alpha 1$ -specific mAb2b antibody (Fig. 2C). The GlyR $\alpha 1$ -positive cells showed morphological peculiarities, such as a spherical shape and reduced adherence (Fig. 2B,C). More strikingly, GlyR $\alpha 1$ protein was detected mainly in the cytosol and nucleus of GL261 cells (Fig. 2B, right-hand high-power view, arrows; supplementary material Table S3), suggesting that GlyRs do not serve as neurotransmitter receptors in these cells. Consistent with the nuclear localization of GlyR $\alpha 1$, GL261 cells expressed importin $\alpha 3$ and $\alpha 4$ mRNA (Fig. 2D), which mediate nuclear import of GlyRs (Melzer et al., 2010).

GlyRs do not form glycine-gated ion channels at the surface of GL261 or human glioma cells

We used the patch-clamp technique to record membrane currents in response to glycine application. To monitor changes in membrane conductance, the membrane potential was repetitively clamped to a series of hyper- and de-polarizing potentials ranging from -120 to $+20$ mV, as described previously for the recording of γ -aminobutyric acid type A receptor ($GABA_A$ R)-dependent Cl^- currents (Labrakakis et al., 1998). GlyR $\alpha 1$ -positive, round shaped and slightly detached GL261 cells were investigated (Fig. 3A), but the membrane conductance was not affected by glycine application (Fig. 3B,C; $n=15$). Likewise, human glioma cells from resected glioblastoma multiforme did not respond to glycine application (TU7/00, supplementary material Fig. S1A, Fig. S3C; $n=15$), despite expression of GlyR $\alpha 1$ - and $\alpha 3$ -encoding mRNA in these cells (supplementary material Fig. S1B–D). GlyR $\alpha 2$ -encoding mRNA was not detected (supplementary material Fig. S1D), whereas GlyR $\alpha 4$ - and β -encoding mRNAs were expressed (supplementary material Fig. S1E). However, these GlyR

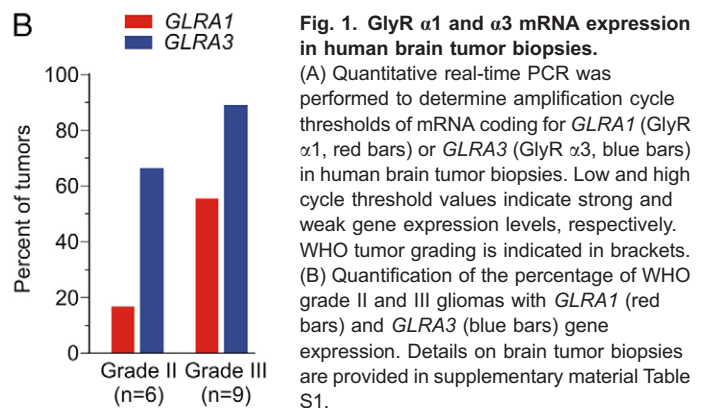
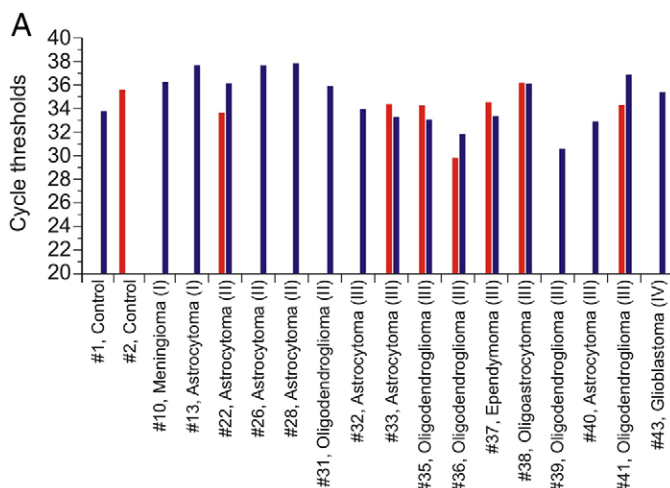


Fig. 1. GlyR $\alpha 1$ and $\alpha 3$ mRNA expression in human brain tumor biopsies.

(A) Quantitative real-time PCR was performed to determine amplification cycle thresholds of mRNA coding for *GLRA1* (GlyR $\alpha 1$, red bars) or *GLRA3* (GlyR $\alpha 3$, blue bars) in human brain tumor biopsies. Low and high cycle threshold values indicate strong and weak gene expression levels, respectively. WHO tumor grading is indicated in brackets. (B) Quantification of the percentage of WHO grade II and III gliomas with *GLRA1* (red bars) and *GLRA3* (blue bars) gene expression. Details on brain tumor biopsies are provided in supplementary material Table S1.

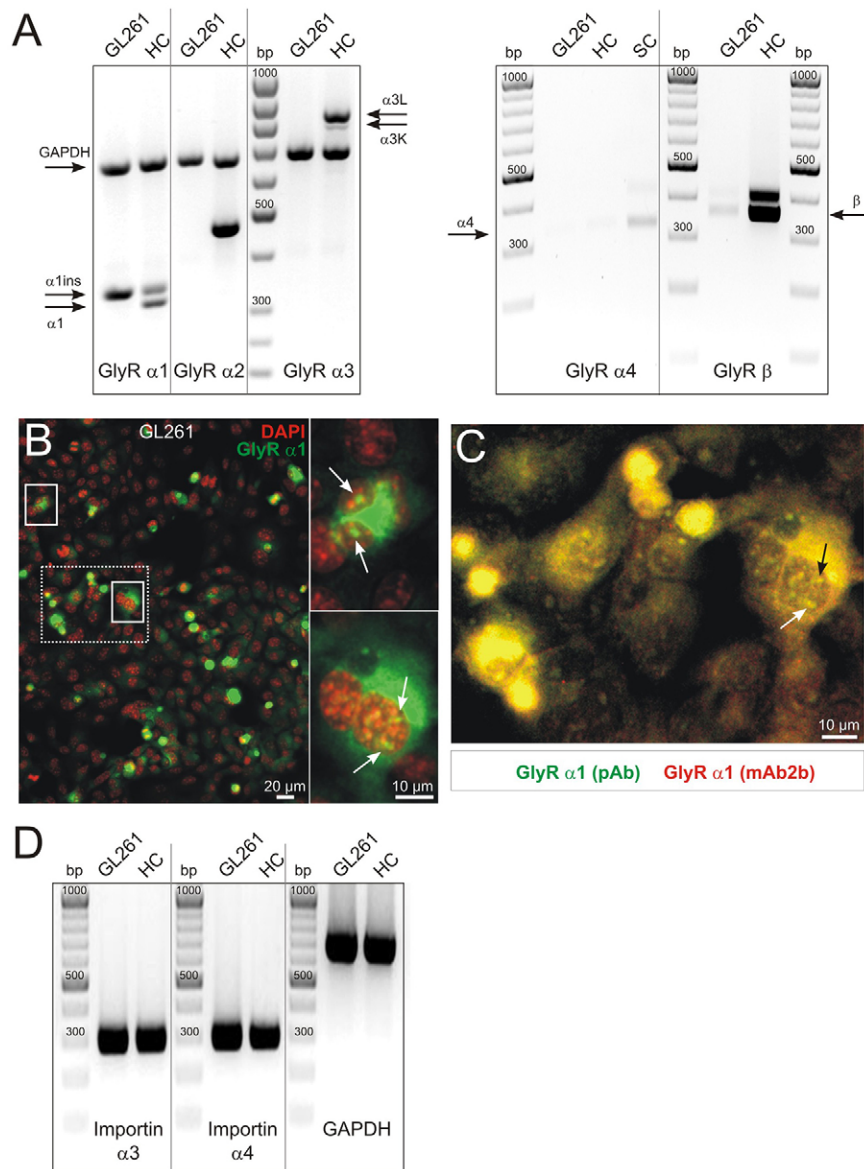


Fig. 2. GlyR $\alpha 1$ and importin expression in mouse GL261 cells. (A,B) Mouse GL261 glioma cells were processed for RT-PCR with oligonucleotides specific to GlyR $\alpha 1$, $\alpha 2$, $\alpha 3$, $\alpha 4$, and β cDNAs. For the GlyR $\alpha 1$ and $\alpha 3$ subunits, PCR products span alternatively spliced regions in the large cytosolic loop domain. To verify presence of mRNA, cDNA coding for the house keeping gene *GAPDH* was co-amplified. Furthermore, as a positive control, mRNA samples obtained from adult mouse hippocampus (HC) or spinal cord (SC) were included. Note that GL261 cells expressed only the 'ins' RNA splice variant of the GlyR $\alpha 1$ subunit. A faint band corresponding to GlyR β was also detected in the GL261 sample. (B,C) Immunofluorescence analysis of GlyR $\alpha 1$ protein expression in GL261 cells using a polyclonal antibody (B,C) and the well-characterized mAb2b antibody (C). Nuclei were visualized using DAPI stain (B). High-power views of the boxed regions are shown on the right (solid boxes) and in C (dashed box) and indicate intranuclear GlyR $\alpha 1$ expression (arrows; see supplementary material Table S3 for values). Also note that the immunofluorescence GlyR $\alpha 1$ signals obtained with two different antibodies are nearly congruent (C). (D) GL261 cells also expressed importin $\alpha 3$ and $\alpha 4$.

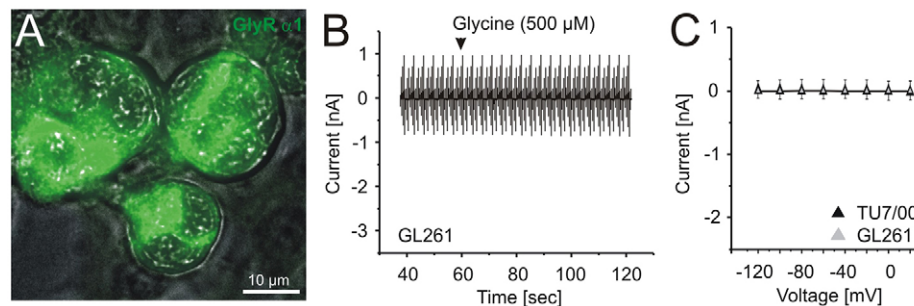


Fig. 3. Neither human nor mouse glioma cells respond to glycine application with transmembrane Cl^- currents. (A,B) GlyR $\alpha 1$ -positive, typically round-shaped, glioma cells (A, example shown for GL261 cells) were selected for patch-clamp analysis. (B) Current profile of an example trace obtained from a round-shaped GL261 cell upon voltage ramps. The arrow marks the onset of glycine application (500 μM). (C) Summary of the current–voltage relationships obtained from recordings of mouse GL261 cells and human GlyR $\alpha 1$ - and $\alpha 3$ -expressing glioma cells (TU7/00, supplementary material Fig. S1) demonstrating failure of glycine application to induce transmembrane Cl^- currents.

subunits will not form functional neurotransmitter receptors at the cell surface of human cells. Thus, despite expression of various ligand-binding α -subunits, which are principally able to generate surface neurotransmitter receptors in human cells, GlyRs do not fulfill this task in mouse or human glioma cells (Fig. 3C). Furthermore, we found that importin $\alpha 3$ and $\alpha 4$ were expressed in the majority of samples derived from glioblastoma multiforme (supplementary material Fig. S1E), suggesting that GlyR subunits with NLSs ($\alpha 1$ and $\alpha 3$) have an intranuclear function in mouse and human glioma cells.

Full-length GlyR $\alpha 1$ ins is expressed in intracellular compartments of glioma cells

Ubiquitin-dependent proteolytic processing of GlyR $\alpha 1$ ins has been shown to release receptor fragments with molecular masses of 35 and 13 kDa, the latter corresponding to the size of large cytosolic loop including transmembrane domain (TM) 4 (Büttner et al., 2001). Hence, we next investigated whether proteolysis is responsible for intracellular GlyR expression in glioma cells (Fig. 4). To this end, we generated a recombinant GlyR $\alpha 1$ ins expression construct with two different epitope tags located in the surface-accessible ligand-binding domain (Fig. 4A, Myc tag) and in the large cytosolic loop domain between transmembrane segments TM3 and TM4 [Fig. 4A, hemagglutinin (HA) tag]. We did not detect receptor protein fragments using an HA-directed antibody in western blot analysis (Fig. 4B). In agreement with the electrophysiological data shown above (Fig. 3), transfected GL261 cells did not show receptor surface labeling, although immunoreactivity of the HA epitope tag clearly revealed recombinant GlyR protein expression in the cytosol and nucleus (Fig. 4C; supplementary material Table S3). For control purposes, we verified that the recombinant GlyRs were able to access the cell surface in HEK293 cells (Fig. 4D). These results show that full-length GlyR $\alpha 1$ ins is retained in intracellular compartments of glioma cells including the nucleus (supplementary material Table S3).

GlyR sequence-intrinsic determinants govern intracellular receptor expression

GlyR $\alpha 1$ and $\alpha 3$ subunits contain functional NLSs (RRKRR and RRKRK, respectively) in the large cytosolic loop domain (Melzer et al., 2010; Winkelmann et al., 2014). In the GlyR $\alpha 2$ subunit, the NLS is disrupted by insertion of glutamine residue (RRRQKR, Fig. 5A). Furthermore, the GlyR $\alpha 1$ and $\alpha 3$ loops contain a di-leucine motif involved in adaptor protein 2 (AP2)-dependent receptor internalization (Huang et al., 2007) upstream of the NLS. In GlyR $\alpha 2$, the di-leucine motif is absent (Fig. 5A). To find out whether the NLS or the di-leucine motif is responsible for intracellular GlyR expression, recombinant GlyR $\alpha 2$ and chimeric GlyR $\alpha 1$ – $\alpha 2$ constructs were generated and expressed in GL261 cells (Fig. 5B–D). Whereas GlyR $\alpha 2$ accessed the surface of transfected GL261 cells (Fig. 5B, Myc), disruption of the di-leucine motif by inserting the corresponding GlyR $\alpha 2$ sequences into GlyR $\alpha 1$ (myc- $\alpha 1$ ins-NLS- Δ LL- $\alpha 2$ -HA, Fig. 5A) was not sufficient for receptor surface expression (Fig. 5C). However, GlyR $\alpha 1$ ins was detected at the cell surface, and it disappeared from the nucleus, upon additional disruption of the NLS (myc- $\alpha 1$ ins- Δ LL- Δ NLS- $\alpha 2$ -HA, Fig. 5A,D; supplementary material Table S3), suggesting that the NLS is responsible for the restriction of GlyR $\alpha 1$ ins to the intracellular compartment of GL261 cells.

To investigate whether intracellular GlyR expression in GL261 is subunit specific or valid for all α -subunits with NLSs, we transfected GL261 cells with a mCherry–GlyR- $\alpha 3$ K fusion construct and performed 3D confocal live-cell receptor imaging to further gather information about the dynamics of intracellular receptor distribution (supplementary material Movies 1–3; Fig. 6). Supplementary material Movies 1 and 2 show two views of the same cell (top and side views). Supplementary material Movie 3 shows another cell. Projected z -stacks of mCherry and Hoechst 33342 fluorescent signals (red and blue, respectively) acquired during 90-min recording intervals (supplementary material Movies 1–3; 30 frames/s with each

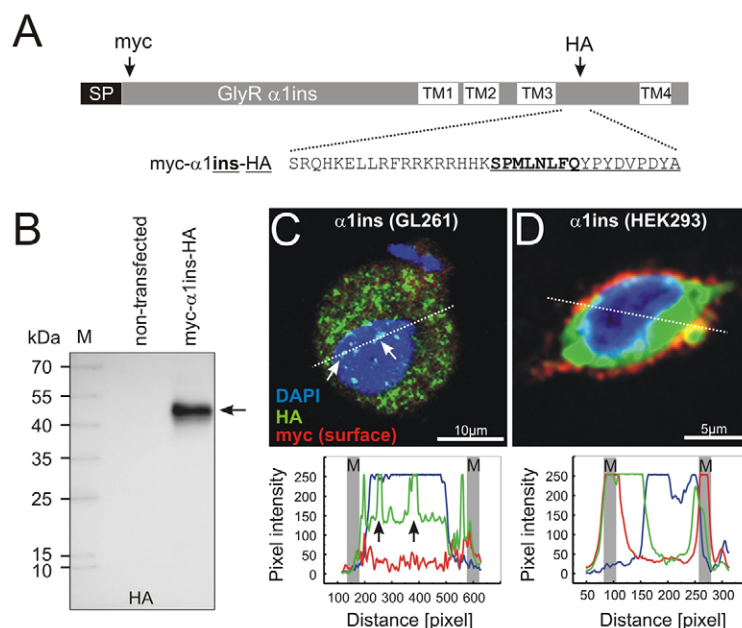


Fig. 4. Full-length GlyR $\alpha 1$ protein is expressed in cytosol and nucleus of GL261 cells. (A) Scheme depicting design of recombinant GlyR $\alpha 1$ ins construct used for investigation of subcellular GlyR distribution, including the cell surface (using the Myc tag) and intracellular compartments (using the HA tag). Positions of the Myc and HA tags are marked with arrows. The zoomed region of the large cytoplasmic loop provides details on the amino acid sequence at the N-terminus of the large cytosolic loop. Sequence of the RNA splice insert 'ins' is highlighted bold and underlined, and the HA tag sequence is shown underlined. SP, signal peptide. (B) Western blot analysis of GlyR myc- $\alpha 1$ ins-HA protein expression in non-transfected and transfected (myc- $\alpha 1$ ins-HA) GL261 cells. A single band (arrow) corresponding to full-length (48 kDa) GlyR Myc- $\alpha 1$ ins-HA protein was detected using the anti-HA antibody, ruling out proteolytic processing of GlyR $\alpha 1$ ins in GL261 cells. M, molecular mass marker. (C) Confocal image of a GlyR myc- $\alpha 1$ ins-HA-expressing GL261 cell. Note that surface accessible Myc tag was not detected using live-cell surface staining, whereas HA immunoreactivity (green) was detected in the cytosol and nucleus (blue) following cell fixation and permeabilization (see supplementary material Table S3 for values). GL261 cell nuclei are shown in blue color. Fluorescence profiles measured along the dashed lines are shown below the image. M, plasma membrane. (D) Confocal image of a GlyR myc- $\alpha 1$ ins-HA-expressing HEK293 cell. GlyR myc- $\alpha 1$ ins-HA was detectable at the cell surface, and HA immunoreactivity was found in cytosol but not nucleus. M, plasma membrane.

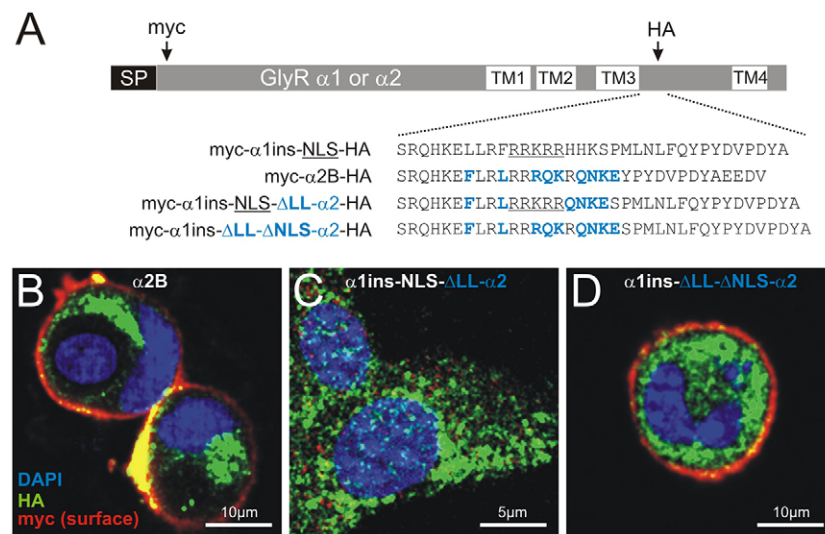


Fig. 5. The NLS region in the $\alpha 1$ subunit is responsible for intracellular GlyR expression in GL261 cells. (A) Scheme depicting design of recombinant GlyR $\alpha 1$ ins or $\alpha 2$ B constructs with a surface-accessible Myc tag, and a HA tag used for staining of the intracellular loop domain. The zoomed region provides details on the amino acid sequence at the N-terminus of the large cytosolic loop including the di-leucine motif up-stream of the NLS in GlyR $\alpha 1$ ins (underlined). GlyR $\alpha 2$ -specific sequence determinants are highlighted with blue color. In chimeric GlyR $\alpha 1$ ins- $\alpha 2$, the di-leucine motif and NLS were disrupted by replacement of the corresponding amino acids in $\alpha 1$ ins with those in $\alpha 2$ (blue). SP, signal peptide. (B–D) Confocal images showing immunochemical signals corresponding to the large cytosolic loop (HA tag, green) and the surface-accessible Myc tag (red) of representative transfected GL261 cells with GlyR myc- $\alpha 2$ B-HA (B), myc- $\alpha 1$ ins-NLS- Δ LL- $\alpha 2$ -HA (C) or myc- $\alpha 1$ ins- Δ LL- Δ NLS- $\alpha 2$ -HA (D). GL261 cell nuclei appear in blue color. Live-cell surface staining with anti-Myc antibody revealed GlyR $\alpha 2$ B expression at the GL261 cell surface (red). Note that GL261 cell nuclei were devoid of HA immunoreactivity. Also note that deletion of the di-leucine motif in GlyR $\alpha 1$ ins was not sufficient to trigger receptor surface expression, whereas additional disruption of the NLS brought the subcellular distribution pattern of GlyR $\alpha 1$ ins more in line with GlyR $\alpha 2$. See supplementary material Table S3 for quantification of nuclear versus somatic distribution of the recombinant GlyR constructs.

frame representing the projection of 10 z -sections, 1- μ m step size) are shown. Individual frames extracted from supplementary material Movie 1 are shown in Fig. 6B and supplementary material Fig. S2. Besides the nuclear localization of GlyR $\alpha 3$ K

(supplementary material Table S3), the live-cell imaging also revealed that $\alpha 3$ K clusters are highly mobile and rapidly shuttle back and forth between cytosol and nucleus (Fig. 6B, arrow, 00:14–00:16 min, and arrowheads, 00:19–00:20 min;

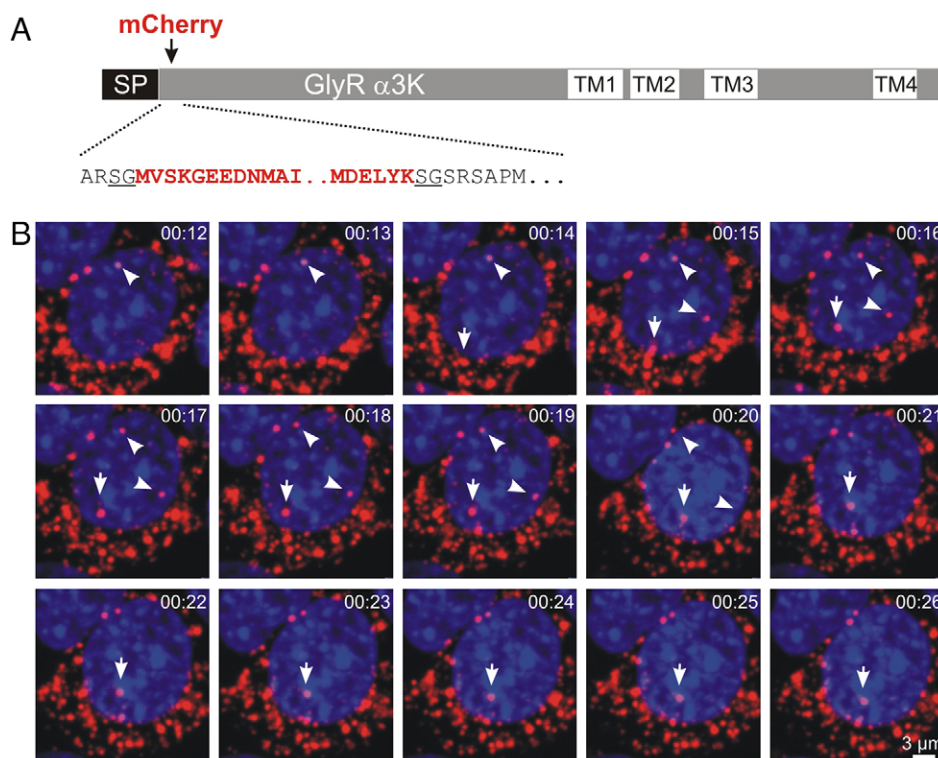


Fig. 6. GlyR $\alpha 3$ also targets to the nucleus of GL261 cells. (A) Scheme depicting design of recombinant GlyR $\alpha 3$ K construct with N-terminal mCherry fluorescent protein used for confocal live-cell GlyR imaging. The zoomed region provides information on the position of mCherry fluorescent protein in GlyR $\alpha 3$ K, which corresponds to the position of Myc tags in GlyR $\alpha 1$ ins and $\alpha 2$ B subunits, following the second amino acid of the mature signal-peptide-cleaved GlyR protein. Owing to insertion of the *BspE1* cloning site, two additional amino acids (underlined) flank the mCherry sequence (red) in the mCherry-GlyR- $\alpha 3$ K construct. SP, signal peptide. (B) Confocal images extracted from supplementary material Movie 1 providing information on the dynamics of intracellular mCherry-GlyR- $\alpha 3$ K (red) distribution during a 15-min recording interval. Nuclei of GL261 cells appear in blue color. Note that $\alpha 3$ K clusters enter (arrows) and exit (arrowheads) the nucleus within a minute, and that $\alpha 3$ K clusters are associated with many sites inside GL261 cell nuclei. For a three-dimensional reconstruction of serial confocal images see supplementary material Fig. S2.

supplementary material Fig. 2B). Intra-nuclear dynamics, however, were much slower and α 3K clusters remained associated with different euchromatin regions for several minutes (Fig. 6B, arrow). Just like GlyR α 1ins (above, Fig. 4C), mCherry–GlyR– α 3K clusters were thus detected at the same time at different euchromatin positions in the GL261 cell nucleus, suggesting that they might influence transcription of different genes. For control purpose, we verified that mCherry–GlyR– α 3K accessed the surface of HEK293 cells by recording glycine-dependent transmembrane Cl^- currents (supplementary material Fig. S3). Collectively, these results show that the NLSs in the large cytosolic loops of full-length α 1ins and α 3K GlyRs mediate cytosolic and intra-nuclear receptor expression specifically in glioma cells.

Knockdown of GlyR expression changes GL261 gene expression

To study functional relevance of intracellular GlyR expression, GlyR α 1ins expression was knocked down in GL261 cells. Stable

knockdown cell lines were obtained by transfection of GL261 cells with GlyR α 1-specific small hairpin RNA (shRNA) constructs ‘G10’ and ‘G11’ (Fig. 7A). Our immunochemical analyses confirmed the shRNA-dependent impact on GlyR α 1 protein expression because ubiquitin-associated perinuclear GlyR α 1 immunoreactivity was detected in G10 and G11 cells (Fig. 7B, α 1-KD-1 and α 1-KD-2). Consistently, the western blot analyses revealed that full-length GlyR α 1ins protein expression was reduced to $36.3\% \pm 1.8$ in α 1-KD-1 and $13.4\% \pm 0.8$ in α 1-KD-2 cells (mean \pm s.d., $n=3$ experiments) compared to the expression level in control GL261 cells (set at 100%). Western blotting against the house-keeping protein α -tubulin served as reference for normalization purpose (Fig. 7C,D). To find out whether intra-nuclear GlyR expression changes gene expression in GL261 cells, we performed quantitative real-time PCR to compare mRNA expression of mouse orthologs of human genes selected by the International Stem Cell Initiative (Adewumi et al., 2007), using the Mouse Stem Cell Pluripotency Array. Reduced GlyR α 1ins protein expression indeed affected the mRNA expression of many

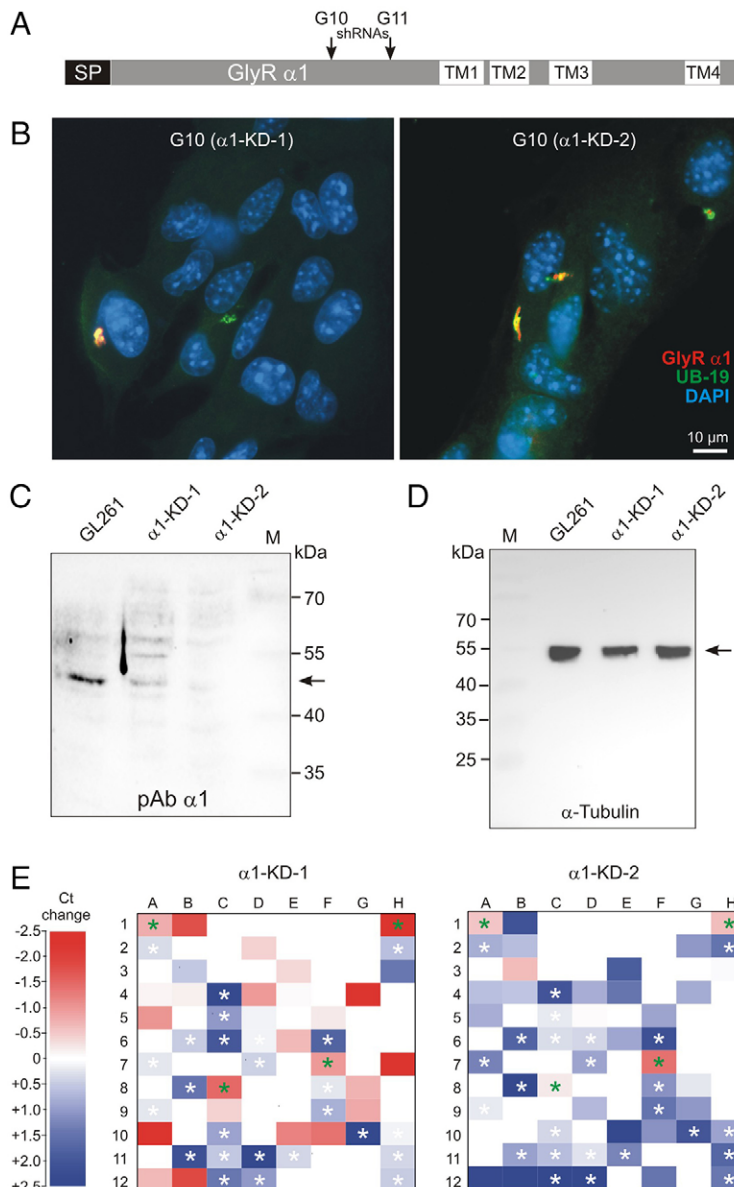


Fig. 7. Knockdown of GlyR α 1ins expression changes gene expression in GL261 cells.

(A) Scheme depicting position of hybridization of the two effective shRNAs, TRC6-G10 (G10) and TRC6-G11 (G11). (B) Immunofluorescence analysis of GlyR α 1 distribution in G10- and G11-knockdown cells. Note that shRNA expression resulted in colocalization of GlyR α 1 with ubiquitin (UB-19) in the perinuclear compartment. (C,D) Western blot analyses of GlyR α 1 and α -tubulin protein in GL261 cells and the GlyR α 1 knockdown cell lines α 1-KD-1 and α 1-KD-2. Bands corresponding to GlyR α 1 (C) and α -tubulin (D) are marked with arrows. (E) The color code represents changes in cycle thresholds (Ct) compared to GL261 cells. Color-coded heat maps show downregulated gene products (blue squares) in both α 1-KD-1 and α 1-KD-2 GlyR α 1ins knockdown GL261 cells. They are marked with white asterisks and mainly belong to the categories ‘signaling pathways’ (*Raf1*, *Gal*, *Grb7*), ‘transcriptional and translational regulation’ (*Eomes*, *Eef1a1*, *Gata4*, *Isl1*, *Olig2* and *Pax6*) and ‘stemness’ (*Bxdc2*, *Cd9*, *Dnmt3b*, *Gata6*, *Gdf3*, *Il6st*, *Kit*, *Ilf1m2*, *Nes* and *Tert*). Upregulated gene products (red squares) were *18S*, *Gcg*, *Pax4* and *TdGF1* (green asterisks).

different genes (Fig. 7E; supplementary material Table S4). Downregulated gene products in both $\alpha 1$ -KD-1 and $\alpha 1$ -KD-2 GlyR $\alpha 1$ ins-knockdown cells included those involved in signaling pathways, including the extracellular-signal-regulated kinase (ERK) (*Gal*, *Grb7*, *Raf1*; Fig. 7E; supplementary material Table S4) and β -catenin/Wnt (proto-oncogene *Ctnnb1*) pathways. Furthermore, mRNA expression of transcriptional regulators (*Eomes*, *Eef1a1*, *Gata4*, *Isl1*, *Olig2*, *Pax6*) and factors that determine self-renewal capacity (*Bxdc2*, *Cd9*, *Dnmt3b*, *Gata6*, *Gdf3*, *Il6st*, *Kit*, *Ifitm2*, *Nes*, *Tert*) were downregulated in the two GlyR knockdown cell lines. Just a few gene products were upregulated (*Gcg*, *Pax4*, *Tdgl1*; Fig. 7E; supplementary material Table S4). These results show that intracellular GlyRs modify expression of genes with tumorigenic potential.

Knockdown of GlyR expression impairs neurosphere formation

To address the possibility that the GlyR-dependent impact on GL261 gene expression affects the self-renewal capacity of GL261 cell, we used the limiting dilution assay, which is an independent predictor of clinical outcome in malignant glioma (Laks et al., 2009). To this end, the different GL261 cell lines were cultured in stem cell medium until the first neurospheres appeared. Then, the minimal number of cells required for neurosphere formation in each well of the culture dish was determined (Fig. 8). A much higher number of the GlyR-knockdown cells as compared to control GL261 cells was required for sphere formation, indicating that neurosphere formation was suppressed in $\alpha 1$ -KD-1 and $\alpha 1$ -KD-2 cells

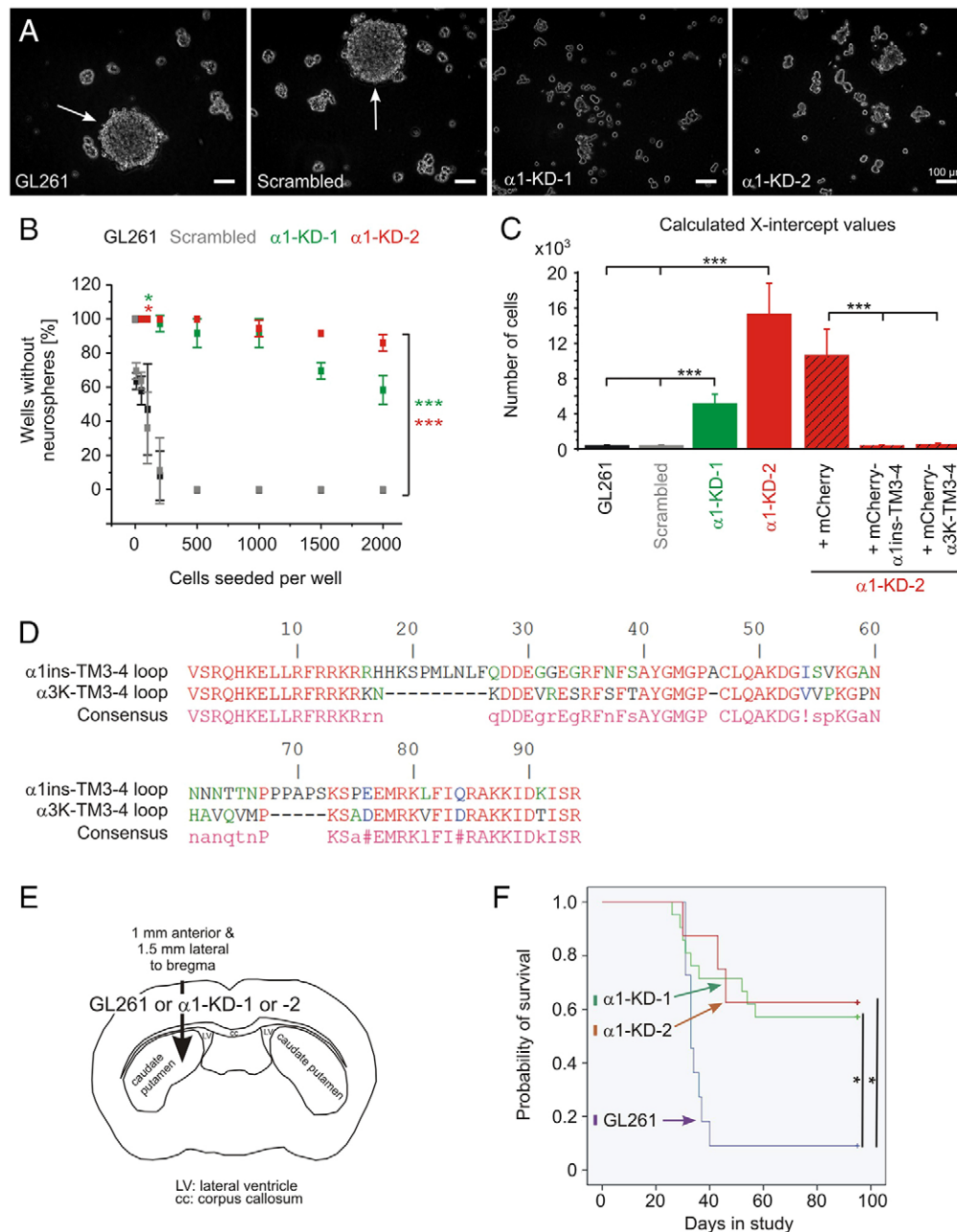


Fig. 8. Knockdown of GlyR $\alpha 1$ ins expression impairs neurosphere and glioma formation. (A–C) For the limiting dilution assay and investigation of the neurosphere-forming capacity, GL261, scrambled shRNA-expressing GL261, $\alpha 1$ -KD-1, $\alpha 1$ -KD-2 cells, and $\alpha 1$ -KD-2 cells expressing mCherry, mCherry- $\alpha 1$ ins-TM3-4 or mCherry- $\alpha 3$ K-TM3-4 were cultured in stem cell medium for 1 week. (A) Images show representative examples of neurosphere formation (arrows) in wells with 1000 seeded cells. (B) Quantification of the percentage of wells without neurospheres per cell plating density (10, 50, 100, 500, 1000, 1500 or 2000 cells per well). Note the strongly reduced sphere-forming capacity of $\alpha 1$ -KD-1 or $\alpha 1$ -KD-2 cells throughout all investigated cell plating densities. (C) Linear regression analysis was performed in order to determine the minimal number of cells per well required for formation of at least one neurosphere (x-intercept value). * $P < 0.05$ (100 cells), *** $P < 0.001$ (all cell plating densities except 100 cells per well), as determined by one-way ANOVA with post-hoc Bonferroni tests. (D) Sequence alignment of GlyR $\alpha 1$ ins and $\alpha 3$ K large cytosolic loops reveal a high degree of similarity. (E) Scheme providing information on stereotaxic injection of GL261, $\alpha 1$ -KD-1 or $\alpha 1$ -KD-2 knockdown cells into the mouse brain. (F) Cumulative survival plot of mice that were inoculated with GL261, $\alpha 1$ -KD-1, or $\alpha 1$ -KD-2 knockdown cells. Note that knockdown of GlyR $\alpha 1$ expression strongly impaired glioma formation *in vivo* as both life span and survival rate of knockdown cell-inoculated mice were increased.

(Fig. 8B,C; x -intercept values, $\alpha 1$ -KD-1, 5137 ± 871 , $\alpha 1$ -KD-2, $15,800 \pm 2880$ versus GL261 control cells, 249 ± 61 ; mean \pm s.e.m.). As a control for the shRNA knockdown strategy, we verified that expression of scrambled shRNA did not influence the capacity of GL261 cells to form neurospheres (x -intercept value of scrambled shRNA-expressing GL261 cells, 247 ± 78 , mean \pm s.e.m.). Importantly, stable expression of the large cytosolic GlyR $\alpha 1$ ins loop between TM3 and TM4 rescued the sphere formation capacity of $\alpha 1$ -KD-2 cells (Fig. 8C, x -intercept value of mCherry- $\alpha 1$ ins-TM3-4-expressing GL261 cells, 280 ± 97 ; mean \pm s.e.m.), which clearly identifies the loop as the relevant GlyR $\alpha 1$ ins signaling domain. Moreover, the large cytosolic GlyR $\alpha 3$ K loop was equally effective in rescuing the self-renewal capacity of $\alpha 1$ -KD-2 cells (Fig. 8C, x -intercept value of mCherry- $\alpha 3$ K-TM3-4-expressing GL261 cells, 365 ± 144 , mean \pm s.e.m.). As a control, we verified that mCherry expressed without GlyR protein domains did not influence the capacity of GL261 cells to form neurospheres (Fig. 8C, x -intercept value of mCherry-expressing $\alpha 1$ -KD-2 cells, $10,519 \pm 3420$, mean \pm s.e.m.). Thus, reduced GlyR $\alpha 1$ ins protein expression impairs the self-renewal capacity of GL261 cells. It is striking, that both GlyR $\alpha 1$ ins and the $\alpha 3$ K large cytosolic loops are able to rescue it and, hence, are two functionally equivalent versions of the relevant signaling domain (Fig. 8D).

Knockdown of GlyR expression impairs glioma formation *in vivo*

In order to find out whether impaired self-renewal capacity would result in reduced tumorigenicity, GL261, $\alpha 1$ -KD-1 and $\alpha 1$ -KD-2 cells were inoculated by stereotactic injection into the caudate putamen of GL261-isogenic wild-type mice (Fig. 8E), and the probability of survival and the lifespan of GL261-cell-inoculated mice were monitored (Fig. 8F). Reduction of GlyR $\alpha 1$ ins protein expression impaired glioma formation *in vivo* as the majority of knockdown-cell-inoculated mice survived without developing tumors [Fig. 8F; 57% (12 of 21) of $\alpha 1$ -KD-1-inoculated mice, and 63% (5 of 8) of $\alpha 1$ -KD-2-inoculated mice]. Furthermore, the lifespan of knockdown-cell-injected mice with tumor formation was significantly prolonged, which suggests that glioma formation was slowed down in those animals that developed tumors despite knockdown of GlyR expression (Fig. 8F). Consistently, post-mortem analysis revealed similarly sized tumors in all animals which died due to GL261 cell inoculation (supplementary material Fig. S4A–C), but with a significant delay in the experimental mouse groups that were inoculated with GlyR-knockdown cells (Fig. 8F). Thus, we also conclude that knockdown of GlyR $\alpha 1$ ins expression impairs tumor progression *in vivo*, which is supported by reduced proliferation rates of $\alpha 1$ -KD-1 and $\alpha 1$ -KD-2 cell lines in cell culture (supplementary material Fig. S4D). Collectively, these results identify a crucial role of intracellular GlyR function for regulation of tumorigenicity and tumor progression.

DISCUSSION

The neurotransmitter glycine has been shown to serve a metabolic role in brain tumor formation (Jain et al., 2012). The high glycine content of brain tumors (Bobek-Billewicz et al., 2010) prompted us to test whether glioma cells express GlyRs to sense the glycine level in the extracellular space. We found, however, that NLS-harboring receptors were not expressed on the cell surface, but rather served a new intracellular signaling function that modified tumor cell gene expression, self-renewal capacity and tumorigenicity.

Mouse GL261 glioma and human stem-cell-like tumor cells preponderantly expressed the GlyR $\alpha 1$ ins and $\alpha 3$ K RNA splice variants, which contain the sequence SPMLNLFQ (Malosio et al., 1991) and lack the splice insert coding for TAEFALEKFYRFSDT (Nikolic et al., 1998), respectively. The protein region where RNA splicing changes amino acid sequences is interesting as it is located immediately downstream of the NLS region. It has been established that this protein region influences GlyR protein structure as, for example, inclusion of exon 8A (coding for TAEFALEKFYRFSDT) changes receptor desensitization kinetics, clustering and subcellular trafficking in neurons (Eichler et al., 2009; Nikolic et al., 1998; Notelaers et al., 2012; Winkelmann et al., 2014). The tumor-cell-specific preponderant expression of GlyR $\alpha 1$ ins and $\alpha 3$ K RNA splice variants identifies a functional role for GlyR $\alpha 1$ ins and sets glioma cells apart from neurons with regard to RNA splicing of GlyR $\alpha 3$ -coding gene transcripts (Eichler et al., 2009). Our results also identify a possible crucial functional role for non-charged amino acids corresponding to the RNA splice insert downstream of the NLS in GlyR $\alpha 1$.

Although it has been established that the monopartite NLS in the large cytosolic GlyR loop domain is able to interact with nuclear import proteins of the karyopherin family (importin $\alpha 3$ and $\alpha 4$) (Melzer et al., 2010), the functional impact of the NLS in GlyR $\alpha 1$ and $\alpha 3$ subunits remained elusive. Western blot analyses of GlyR-transfected GL261 cells revealed that nuclear GlyR expression was not due to release of GlyR protein fragments upon proteolysis. This is distinct to other transmembrane receptors, which are known to require release of proteolytic protein fragments for activation of intracellular signaling domains (Hollmén et al., 2012; Nanba et al., 2003). Our experiments with chimeric GlyR constructs furthermore showed that deletion of the di-leucine motif involved in receptor internalization (Huang et al., 2007) was not sufficient to change the subcellular receptor distribution in GL261 cells. In support of a crucial role for the NLS region, additional deletion of the NLS in GlyR $\alpha 1$ was sufficient to enable receptor surface expression in GL261 cells. Although we cannot rule out a possible contribution of the β subunit (Fig. 2A; supplementary material Fig. S1E) to the peculiar subcellular GlyR trafficking in glioma cells (Del Pino et al., 2014), our data present evidence for a crucial role of the NLS region in the intracellular GlyR function discovered in this study.

In agreement with the established membrane topology of full-length GlyRs (Breitinger and Becker, 2002; Zuleger et al., 2012), the large cytosolic loop domain between transmembrane segments 3 and 4 of intranuclear GlyRs will be exposed to genomic DNA in the nucleoplasm of glioma cells. In fact, Cys-loop neurotransmitter receptors have a common origin (Tasneem et al., 2004), and our BLAST search of the NCBI prokaryote database revealed substantial ($\sim 30\%$) similarity between the large cytosolic GlyR loop domain encoded by exon 9 and prokaryotic proteins with molecular chaperone function (proteasome-activating nucleotidase, sequence ID: gb|ADD93104.1) or DNA-processing activity (type III restriction protein res subunit, sequence ID: gb|EMA60229.1). Furthermore, we recently presented evidence for co-sedimentation of GlyR large cytosolic loops with RNA-binding proteins and proteins that regulate transcription [e.g. heterogeneous nuclear ribonucleoprotein K (*Hnrpk*) or transcriptional activator protein Pura (*Pura*) (see Winkelmann et al., 2014)]. In agreement with an evolutionarily conserved role of exons in exon-shuffled contemporary genes in mammals, it is tempting to speculate that

the functional impact of NLS-harboring GlyRs in glioma cells involves regulation of gene expression. Our quantitative PCR analysis of the Mouse Stem Cell Pluripotency Array (Adewumi et al., 2007) indeed supports this idea as it identified a set of GlyR target genes. Most of them belong to the category ‘stemness’ (*Bxdc2*, *Cd9*, *Dnmt3b*, *Gata6*, *Gdf3*, *Il6st*, *Kit*, *Ifitm2*, *Nes*, *Tert*) and are good candidates for the genes that are responsible for the impaired self-renewal capacity of α 1-KD-1 and α 1-KD-2 cells in the neurosphere formation assay and the reduction in the initiation of glioma formation by GlyR α 1ins knockdown GL261 cells in the experimental mouse model. Although the exact signaling mechanisms of the GlyR-dependent impact on GL261 gene expression remain to be determined, our study identifies an intriguing strategic (possibly gene regulatory) role for the NLS-harboring large cytoplasmic loop domain of GlyRs in glioma cells. That both GlyR α 1ins and α 3K large cytosolic loop domains were able to rescue self-renewal capacity of GlyR α 1ins knockdown GL261 cells indeed demonstrates functional equivalence of these protein domains. In fact, the large cytosolic loops of GlyR α 1ins and α 3K share 60% sequence similarity (Combet et al., 2000). Thus, the identified GlyR protein regions and their consensus sequence (Fig. 8D) might be relevant for tumor therapy as they could be functionally neutralized using cell-penetrating peptides that specifically target glioma cells through proteolytic activation (Jiang et al., 2004) in patients with GlyR α 1- and/or α 3-positive brain tumors.

In summary, our study determines the GlyR α 1ins and α 3K large cytosolic loops as glioma-cell-specific and tumorigenic intracellular receptor signaling domains. These results make a strategic contribution to the field by revealing a new intracellular and gene regulatory GlyR function that goes much beyond the well-established role of the protein as a neuronal Cys-loop neurotransmitter receptor.

MATERIALS AND METHODS

Analysis of resected brain tumors was performed according to the rules laid down by the Ethical Committee (Charité, EA4-098-11), and informed consent was obtained according to the Declaration of Helsinki (2000). Animals were treated according to the permit given by the Office for Health Protection and Technical Safety of the regional government of Berlin (LaGeSo, TVV 230/05), in compliance with regulations laid down in the European Community Council Directive.

GlyR expression constructs

Recombinant GlyR α 1ins and α 2B expression constructs with surface accessible Myc and intracellular HA epitope tags were generated using site-directed mutagenesis, following the GeneEditor protocol (Promega, Mannheim, Germany). The Myc tag was inserted between the second and third amino acid of the mature, signal peptide cleaved, receptor proteins. The mCherry–GlyR– α 3K construct for confocal live-cell imaging was obtained likewise by inserting a *BspE1* restriction site at this position and in-frame cloning of mCherry-coding sequence. To generate GlyR mCherry– α 1ins-TM3-4 and mCherry– α 3K-TM3-4 loop constructs for the production of Zeocin-resistant stable cell lines, standard molecular cloning procedures were used for their cloning into the pTRACER vector (Clontech). In fusion constructs, the loop domains started with ‘VSK’ and ended with ‘ISR’ followed by linker ‘GPVAT’ (α 1ins) or ‘PVAT’ (α 3K) and the mCherry-coding sequence. In addition, because GL261 cells already express EGFP, the EGFP-coding sequence in the Zeocin-resistance cassette was excised using fusion PCR. Corresponding cDNA clones (Legendre et al., 2009) served as PCR templates. All constructs were verified by DNA sequencing.

Resected brain tumors and cell lines

Resected brain tumors were provided by the Department for Neurosurgery Charité Universitätsmedizin Berlin. Brain tumor material for RT-PCR analysis of GlyR expression was obtained from four patients (TU4/01, primitive neuroectodermal tumor; TU3/01, TU4/06 and TU7/00, glioblastoma multiforme, WHO grade IV), and corresponding cell lines were produced by culturing the dissociated tumor cells in Dulbecco’s Modified Eagle Medium (DMEM; #41965, Invitrogen Life Technologies, Carlsbad, CA) supplemented with 10% FCS, 2 mM L-glutamine, 100 U/ml penicillin and 100 μ g/ml streptomycin at 37°C and under 5% CO₂, as described previously (Labrakakis et al., 1998). The EGFP-expressing high-grade astrocytoma cell line GL261 (Walzlein et al., 2008) (which is isogenic to C57BL/6 mice; National Cancer Institute, Frederick, MD) was used throughout and cultured as shown above or in stem cell medium [2% B27, 100 U/ml penicillin, 100 μ g/ml streptomycin, 20 ng/ml FGF-2, 20 ng/ml EGF in DMEM supplemented with F-12 (Invitrogen Life Technologies)].

Transfection of GL261 cells was carried out using an Amaxa Nucleofector system (kit V, program V001; Lonza, Basel, Switzerland). GlyR α 1-knockdown cell lines were obtained by electroporation of 3×10^6 to 5×10^6 GL261 cells with 2 μ g of the shRNA expression constructs directed against GlyR α 1 (TRC6-G10 and TRC6-G11) or containing scrambled shRNA sequences (Open Biosystems, Huntsville, AL), as a control. To select and maintain stable shRNA-expressing GL261 cells, 0.8 μ g/ μ l puromycin was added to the culture medium. Two stable GlyR α 1 knockdown cell lines were obtained with shRNAs TRC6-G10 and TRC6-G11, which are referred to here as α 1-KD-1 and α 1-KD-2. Stable α 1-KD-2 cell lines expressing mCherry, or constructs encoding the mCherry– α 1ins-TM3-4 loop or the mCherry– α 3K-TM3-4 loop were obtained following nucleofection using program U030 and selection with additional Zeocin antibiotic at a concentration of 300 μ g/ml. mCherry fluorescence was monitored throughout the experiments (not shown). For immunocytochemistry, GL261 cells were transfected with GlyR-coding plasmids using the Amaxa Nucleofector system as described above, but applying the program U020. Transfection of GL261 with the mCherry–GlyR– α 3K construct for confocal live-cell imaging was conducted with magnetofect-nano (0.24 μ g DNA, 0.82 μ l nano particles, 1 Hz, 0.2 mm displacement, 1 h; nanoTherics Ltd, Keele, UK). For this purpose, cells were seeded in 24-well plates at an initial cell density of 30,000 cells per well 1 day before transfection, dissociated with trypsin and re-seeded at 1:1 into 35-mm glass-bottomed microwell dishes (MatTek, Ashland, MA) at 1 day post transfection. Live-cell imaging was performed at 4 days post transfection.

Human embryonic kidney cells (HEK293) were cultured as described above and transfected using a standard Ca²⁺/phosphate protocol. At 2 to 3 days after transfection, cells were processed for electrophysiology, immunochemistry or live-cell imaging.

Neurosphere formation in the limiting dilution assay

For the limiting dilution assay, cells were cultured in stem cell medium until primary sphere formation was noted. Cells were then dissociated and plated in 96-well plates in 0.2 ml volumes of stem cell medium. Final cell dilutions ranged from 2000 cells/well to 10 cells/well in 0.2 ml volumes. Twelve wells were seeded per cell plating density. Cultures were fed 0.025 ml of stem cell medium every 2 days until day 7, when the percentage of wells not containing spheres for each cell plating density was calculated and plotted against the number of cells per well. Regression analysis was performed to extract x-intercept values, which represent the number of cells required to form at least one neurosphere in every well.

Inoculation of GL261 cells into the mouse brain

Female wild-type C57Bl/6 mice were purchased from Charles River Laboratories (Sulzfeld, Germany) or bred at the local animal facility. Mouse GL261 control or GlyR α 1-knockdown cells (α 1-KD-1 and α 1-KD-2) were suspended in MEM Eagle with Earle’s BSS supplemented with vitamin B12 (0.25 μ M) and B27 supplement (20 μ l/ml; both Invitrogen), and 1 μ l of cell suspension (2×10^4 cells/ μ l) was injected into

the caudate putamen region (1 mm anterior and 1.5 mm lateral to the bregma, as described previously (Glass et al., 2005).

Electrophysiology

For patch-clamp experiments, extracellular and intracellular solutions were as described previously (Labrakakis et al., 1998). Briefly, extracellular solution contained (in mM) NaCl (150), KCl (5.4), HEPES (5), glucose (10), CaCl₂ (2) and MgCl₂ (1). The pH was adjusted to 7.4 with KOH. Patch pipettes were pulled from a borosilicate glass tube (Hilgenberg GmbH, Malsfeld, Germany) with a horizontal puller (Sutter Instruments, Novato, CA), electrode resistance was 6–8 MΩ. Pipette solution contained (in mM) KCl (130), EGTA (5), HEPES (10), CaCl₂ (0.5), MgCl₂ (2) and ATP (3). Patch-clamp experiments were performed at room temperature. Membrane current recording and voltage stimulation were performed with a patch-clamp amplifier (EPC9 or EPC9/2, HEKA Elektronik, Lambrecht, Germany) and traces were acquired with a 3.0 kHz Bessel filter. Bath application of a nearly saturating glycine concentration (500 μM) was performed 30 s after the baseline current at the holding potential of –60 mV had stabilized. To obtain current voltage curves, the membrane was clamped to a series of depolarizing and hyperpolarizing voltage steps from the holding potential (–120 mV to +20 mV, step size: 20 mV, step duration: 200 ms, duration between steps: 300 ms). In each set of experiments we compared the inward currents prior to glycine application with the ones recorded 15 s after glycine application. The latter corresponds to the time point at which glycine-evoked responses usually peaked in GlyR α1-transfected HEK293 control cells. Average conductance was calculated by linear interpolation of voltage steps between –120 mV and +20 mV. For patch-clamp recording of HEK293 cells, extracellular solution contained (in mM) NaCl (140), KCl (5), HEPES (10), glucose (10), CaCl₂ (2), and MgCl₂ (1). The pH was adjusted to 7.4 with NaOH. Patch pipettes were pulled from a borosilicate glass tube (1B150F-4; World Precision Instruments, Berlin, Germany) with a horizontal puller (Sutter Instruments, Novato, CA), and had resistances of 3–6 MΩ when filled with internal solution. Pipette solution contained (mM) CsCl (130), NaCl (5), CaCl₂ (0.5), MgCl₂ (1), EGTA (5) and HEPES (30), pH was adjusted to 7.2 with CsOH. Cells were clamped at –50 mV and current–voltage (*I–V*) relations were obtained from voltage ramps from –100 mV to +100 mV with a duration of 400 ms applied every 5 s. Traces were recorded with a List EPC7 amplifier and Patchmaster software. Data were sampled at 10 kHz and filtered online at 2.83 kHz (10 kHz + 3 kHz Bessel). HEK cells (500,000) were seeded onto 35-mm dishes 3 days before, and transfected 1 day before measurement with 2 μg plasmid DNA (containing either mCherry-GlyRα3K) and Fugene HD® (Promega, Mannheim, Germany) according to the manufacturer's instructions. At 1–5 h prior to the recording, transfected HEK293 cells were split 1:6 onto glass coverslips and identified according to mCherry fluorescence, which was acquired under a 40× objective using a 16-bit cooled CCD camera (Spot PURSUIT, Visitron Systems GmbH, Puchheim, Germany).

RNA isolation, cDNA synthesis and PCR

RNA was isolated from cultured cells using TRIzol Reagent (Invitrogen). cDNA was obtained by reverse transcription of 2 μg RNA with an equimolar mixture of 3'-anchored poly(T) oligonucleotides (T₁₈V, T₁₅V, T₁₃V) and Superscript II (Invitrogen), according to the manufacturer's protocol.

For PCR amplification of cDNA obtained from human glioma cells, oligonucleotides binding to specific sequences of GlyR α1 (5'-CAGTTTGCTGCTCTTGTGT-3' and 5'-GTTGAAAATGAGGAAGGCCATG-3'), α2 (5'-ATCAACAGTTTGGATCAGTCA-3' for the α2A splice variant or 5'-TCAACAGCTTTGGGTCAATAG-3' for α2B and 5'-CCTTCAGCACTGCCTGACTGG-3' for both) and α3 (5'-GGGTACACAATGAATGATCTC-3' and 5'-AGAGACTTAATCTTGCTGCTGATG-3') were designed as described previously (Eichler et al., 2008; Eichler et al., 2009; Meier et al., 2002) and used in combination with GAPDH-specific primers (5'-ATGGCACCGTCAAGGCTGAG-3' and 5'-CGACGCCTGCTCACCACC-3') (Eichler et al., 2009). The ratio between GlyR α- and GAPDH-specific oligonucleotides was

adjusted to 15:1 (α1 and α2) and 20:1 (α3). For detection of the α4 subunit, oligonucleotides 5'-AGCATAAAGAATTCATACGACTTC-GA-3' and 5'-TGGATATCTTCTGACCATAGCACT-3' were used. The β subunit was detected using oligonucleotides 5'-TGAGCAA-GCAGATGGGAAAGG-3' and 5'-TAACGTTGAAGAACAAGAAG-CAG-3'. Specific oligonucleotides were used for detection of importin α3 (5'-GATGGTTATTGATTCAGGGGTTGTAC-3' and 5'-GATGATAATCATAGGGATTAACCCA-3') and importin α4 (5'-GATGGTATAGACTCTGGCATAGTTC-3' and 5'-GGTGTATTATCATTGTACAAGATTG-3'). RedTaq DNA polymerase (Sigma-Aldrich, Deisenhofen, Germany) and manual hot start were applied, and 40 cycles (1 min annealing at 58°C and 1 min elongation at 72°C) were run. For the purpose of control of oligonucleotides and the PCR protocol, human post-mortem hippocampus RNA (pool of 20 healthy Caucasians) was purchased from Clontech and included in PCR.

cDNA of mouse GL261 glioma cells was screened as described above, except that oligonucleotides specific to mouse GlyR α1 (5'-CTGTTTGCTGCTCTTCTGCTGT-3' and 5'-TGGGAAACCGATGCGAGATA-3'), α2 (5'-ACCGAGTGAATATTTTTCT GAGAC-3' and 5'-GTGAAACTTGACCTCAATGCAG-3'), α3 (5'-GGGTACACAA-TGAATGATCTC-3' and 5'-AGAGACTTAATCTTGCTGCTGATG-3'), α4 (5'-AGCATAAGGAATTTATGAGACTTCGA-3' and 5'-TGGATATCTTCTGACCTTAGTACT-3'), β (5'-TGAGCAAGCAGATGGGAAAGG-3' and 5'-TAACGTTGAAGAACAAGAAGCAG-3'), importin α3 (5'-GATGGTTATTGATTCAGGGGTTGTAC-3' and 5'-GATGATAATCATAGGGATTAACCCA-3') and importin α4 (5'-GATGGTAAATGAGACTCTGGCATAGTTC-3' and 5'-GGTGTATTATCATTGGTACAAGATTG-3') were used. GAPDH-specific primers (5'-CCACTCACGGCAAATTCACG-3' and 5'-AGCCCAAGATGCCCTTCAGTG-3') were included, and again, the ratio between GlyR α- and GAPDH-specific oligonucleotides was adjusted to 15:1 (α1 and α2) and 20:1 (α3). A total of 35 cycles (1 min annealing at 54°C and 1 min elongation at 72°C) were run. For the purpose of control of oligonucleotides and the PCR protocol, adult mouse hippocampus RNA was processed accordingly.

Quantitative real-time PCR, human brain cancer tissue and the mouse stem cell pluripotency array

A β-actin-normalized cDNA panel of pathologist-verified human brain tumors (OriGene Technologies, Inc., Rockville, MD, USA) was used to probe for *GLRA1*, *GLRA2*, and *GLRA3* gene transcript levels by quantitative real-time PCR. The following TaqMan Gene Expression Assays (Applied Biosystems, Foster City, CA, USA) were used: *GLRA1_Hs00609267_m1*, *GLRA2_Hs01033736_m1* and *GLRA3_Hs00197920_m1*. Quantitative real-time PCR was performed according to the TaqMan Gene Expression Assay protocol using the iCycler IQ 5 multicolor real-time detection system (Bio-Rad, Munich, Germany). cDNAs obtained from GL261 control or GlyR α1 knockdown cells (α1-KD-1 and α1-KD-2) were analyzed in a TaqMan Mouse Stem Cell Pluripotency Array (Invitrogen #4414080) using a 7500 real-time PCR system with SDS Software and TaqMan universal PCR master mix (Applied Biosystems, Foster City, CA, USA) according to the manufacturer's instructions. Data were acquired for 40 cycles (cut-off).

Western blotting

Western blot was performed for verification of GlyR protein expression in GL261 cells and quantification of GlyR α1 knockdown in α1-KD-1 and α1-KD-2 cells. Cells were homogenized in the presence of lysis buffer (1% CHAPS, 10 μM pepstatin, 10 μM leupeptin, 0.52 μM aprotinin and 200 μM PMSF in PBS) and centrifuged for 15 min at 4°C and full speed (16,100 g). The protein concentration was determined using the Warburg–Christian equation [$1.55 \times (A_{280} - A_{320}) - 0.76 \times (A_{260} - A_{320})$], where A is the absorbance at the given wavelength, after measuring the extinction with a standard Eppendorf BioPhotometer. Proteins were supplemented with 5× SDS sample buffer containing 50% glycerol, 3.5% SDS, 15% β-mercaptoethanol and 0.02% Bromphenol Blue and boiled for 7 min at 95°C. A total of 8 μg protein per lane was loaded on a 10% SDS gel and run for 1 h at 35 mA (Mini-PROTEAN Tetra System,

Bio-Rad Laboratories, Hercules, CA). Proteins were blotted on a nitrocellulose membrane (0.45 μm , Bio-Rad Laboratories) for 1 h at 2 mA/cm². After blotting, the membrane was washed once with TBST buffer (100 mM Tris-HCl pH 7.4, 154 mM NaCl, and 0.1% Tween 20) and then blocked with 5% goat or donkey serum in TBST for at least 1 h at room temperature. Three TBST wash steps were performed before the membrane was incubated overnight at 4°C with rabbit polyclonal anti- α 1-GlyR antibody (pAb α 1, 1:1000, Chemicon), rat monoclonal anti-HA antibody (clone 3F10, 1:1000, Roche Applied Science, Mannheim, Germany) or rabbit polyclonal anti- α -tubulin antibody (1:1000, Cell Signaling Technology). The secondary horseradish peroxidase (HRP)-conjugated antibodies (1:10,000, Jackson ImmunoResearch Laboratories, West Grove, PA) were applied after four wash steps in TBST and incubated for 90 min at room temperature. After three final wash steps in TBST, signal detection was performed using Immuno-StarTM WesternCTM Chemiluminescence in combination with Molecular Imager ChemiDoc XRS System (Bio-Rad Laboratories).

Immunocytochemistry

For analysis of GL261-endogenous GlyR α 1 protein, cells were fixed for 10 min at -20°C with a mixture (95:5) of methanol and glacial acetic acid and then processed for immunocytochemistry with a rabbit polyclonal antibody (1:300, Abcam, Cambridge, MA, USA) or the well-characterized mouse mAb2b antibody (1:100, Synaptic Systems). For detection of the surface-accessible Myc tag, the mouse monoclonal 9E10 antibody (1:100, Sigma) was used. For this purpose, the 9E10 antibody was applied directly to the cell culture and incubated for 10 min at 37°C in incubator, washed three times with culture medium, fixed as described previously (Meier and Grantyn, 2004; Kowalczyk et al., 2013) and then processed for immunocytochemistry using the rat monoclonal 3F10 antibody (1:200, Roche Applied Science, Mannheim, Germany). Ubiquitin immunoreactivity was assessed using a polyclonal antibody (UB N-19) made in goat (1:100, Santa Cruz Biotechnology, Heidelberg, Germany). Following three wash steps, affinity-purified secondary donkey antibodies coupled to carboxymethyl indocyanine (Cy5) or fluorescein isothiocyanate (FITC) were used. The secondary antibodies were purchased from Jackson ImmunoResearch Laboratories (West Grove, PA, USA).

Microscopy and live-cell imaging

Fluorescent signals were acquired using the laser-scanning confocal microscope DM TCS SP5 (Leica Microsystems). Fluorochromes were excited sequentially to minimize cross-talk between fluorescent signals. Fluorescence was acquired using a HCX PL APO 40 \times UV oil objective (Leica Microsystems). Images were acquired using LCS software (Leica Microsystems) by multiple scanning and averaging of lines (eight times each). Live-cell imaging with confocal microscopy was performed likewise, except that multiple scanning was reduced to three frames per image. Cell nuclei and GlyR α 3K were visualized using Hoechst 33342 (Invitrogen) and mCherry fluorescence, respectively. Optical sections were obtained along the z-axis using a 1- μm step size. Frames were acquired every minute. Movies were created using the software Imaris x64 7.6 (Bitplane Scientific Software, Zurich, Switzerland) and exported at a frame rate of 30 frames/s. For quantification of nuclear versus somatic GlyR distributions, integrated signal intensities were measured cell-wise within circular regions of interest (10 μm diameter) which were nucleus-centered and placed in the perinuclear cytoplasm as described previously (Winkelmann et al., 2014).

Statistics

Statistical analysis of tumor-cell-inoculated mice [Kaplan–Meier survival-analysis, followed by log rank (Mantel–Cox), Breslow (generalised Wilcoxon) and Tarone–Ware test] was performed using the SPSS Statistics software (Predictive Analysis Software 18, SPSS Inc., IBM Company Headquarters, Chicago, IL). One-way ANOVA analysis followed by post hoc Bonferroni test was used for statistical analysis of the subcellular GlyR distribution in GL261 cells. $P < 0.05$ was considered significant.

Acknowledgements

We thank Anje Sporbert (Joint Intravital Microscopy and Imaging platform JIMI) for support and access to the SP5 confocal microscope, and Christina Eichhorn (SPSS & Statistik, IT, Max Delbrück Center for Molecular Medicine, Berlin, Germany) for performing statistical analyses with the SPSS software. We also thank Carola Bernert, Josephine Grosch, Anne Schäfer, Silke Dusatko and Andra Eisenmann at the Max Delbrück Center for Molecular Medicine for excellent technical assistance.

Competing interests

The authors declare no competing interests.

Author contributions

J.C.M. conceived the study. B.F., O.D.a.D., and A.W. performed the majority of the experiments. M.Semtner and B.B. performed electrophysiological experiments. D.S.M., M.Synowitz and R.G. contributed to tumor inoculation. P.W. and M.F. helped with experiments related to analysis of gene expression. M.-P.J. provided the human stem-cell-like cell samples. J.C.M., B.F. and H.K. wrote the paper.

Funding

This study was supported by the Helmholtz Association [grant number VH-NG-246 to J.C.M.]; the Deutsche Forschungsgemeinschaft (DFG) [grant number SFB-TR3, project B5 to J.C.M.]; and the Bundesministerium für Bildung und Forschung (BMBF) [grant number ERA-Net NEURON II, project CIPRESS to J.C.M.].

Supplementary material

Supplementary material available online at <http://jcs.biologists.org/lookup/suppl/doi:10.1242/jcs.146662/-DC1>

References

- Adewumi, O., Aflatoonian, B., Ahrlund-Richter, L., Amit, M., Andrews, P. W., Beighton, G., Bello, P. A., Benvenisty, N., Berry, L. S., Bevan, S. et al.; International Stem Cell Initiative (2007). Characterization of human embryonic stem cell lines by the International Stem Cell Initiative. *Nat. Biotechnol.* **25**, 803–816.
- Bobek-Billewicz, B., Hebda, A., Stasik-Pres, G., Majchrzak, K., Zmuda, E. and Trojanowska, A. (2010). Measurement of glycine in a brain and brain tumors by means of 1H MRS. *Folia Neuropathol.* **48**, 190–199.
- Breitinger, H. G. and Becker, C. M. (2002). The inhibitory glycine receptor-simple views of a complicated channel. *ChemBioChem* **3**, 1042–1052.
- Büttner, C., Sadtler, S., Leyendecker, A., Laube, B., Griffon, N., Betz, H. and Schmalzing, G. (2001). Ubiquitination precedes internalization and proteolytic cleavage of plasma membrane-bound glycine receptors. *J. Biol. Chem.* **276**, 42978–42985.
- Combet, C., Blanchet, C., Geourjon, C. and Deléage, G. (2000). NPS@: network protein sequence analysis. *Trends Biochem. Sci.* **25**, 147–150.
- Del Pino, I., Koch, D., Schemm, R., Qualmann, B., Betz, H. and Paarmann, I. F. (2014). Proteomic analysis of glycine receptor β subunit (GlyR β)-interacting proteins: evidence for syndapin I regulating synaptic glycine receptors. *J. Biol. Chem.* **289**, 11396–11409.
- den Eynden, J. V., Ali, S. S., Horwood, N., Carmans, S., Bröne, B., Hellings, N., Steels, P., Harvey, R. J. and Rigo, J. M. (2009). Glycine and glycine receptor signalling in non-neuronal cells. *Front Mol. Neurosci.* **2**, 9.
- Eichler, S. A., Kirischuk, S., Jüttner, R., Schaefermeier, P. K., Legendre, P., Lehmann, T. N., Gloveli, T., Grantyn, R. and Meier, J. C. (2008). Glycinergic tonic inhibition of hippocampal neurons with depolarizing GABAergic transmission elicits histopathological signs of temporal lobe epilepsy. *J. Cell. Mol. Med.* **12**, 2848–2866.
- Eichler, S. A., Förstera, B., Smolinsky, B., Jüttner, R., Lehmann, T. N., Fähring, M., Schwarz, G., Legendre, P. and Meier, J. C. (2009). Splice-specific roles of glycine receptor α 3 in the hippocampus. *Eur. J. Neurosci.* **30**, 1077–1091.
- Galan-Moya, E. M., Le Guellec, A., Lima Fernandes, E., Thirant, C., Dwyer, J., Bidere, N., Couraud, P. O., Scott, M. G., Junier, M. P., Chneiweiss, H. et al. (2011). Secreted factors from brain endothelial cells maintain glioblastoma stem-like cell expansion through the mTOR pathway. *EMBO Rep.* **12**, 470–476.
- Glass, R., Synowitz, M., Kronenberg, G., Walzlein, J. H., Markovic, D. S., Wang, L. P., Gast, D., Kiwit, J., Kempermann, G. and Kettenmann, H. (2005). Glioblastoma-induced attraction of endogenous neural precursor cells is associated with improved survival. *J. Neurosci.* **25**, 2637–2646.
- Grudzinska, J., Schemm, R., Haeger, S., Nicke, A., Schmalzing, G., Betz, H. and Laube, B. (2005). The beta subunit determines the ligand binding properties of synaptic glycine receptors. *Neuron* **45**, 727–739.
- Harvey, R. J., Schmieden, V., Von Holst, A., Laube, B., Rohrer, H. and Betz, H. (2000). Glycine receptors containing the alpha4 subunit in the embryonic sympathetic nervous system, spinal cord and male genital ridge. *Eur. J. Neurosci.* **12**, 994–1001.
- Hollmén, M., Liu, P., Kurppa, K., Wildiers, H., Reinvald, I., Vandoorpe, T., Smeets, A., Deraedt, K., Vahlberg, T., Joensuu, H. et al. (2012). Proteolytic processing of ErbB4 in breast cancer. *PLoS ONE* **7**, e39413.

- Huang, R., He, S., Chen, Z., Dillon, G. H. and Leidenheimer, N. J. (2007). Mechanisms of homomeric alpha1 glycine receptor endocytosis. *Biochemistry* **46**, 11484–11493.
- Jain, M., Nilsson, R., Sharma, S., Madhusudhan, N., Kitami, T., Souza, A. L., Kafri, R., Kirschner, M. W., Clish, C. B. and Mootha, V. K. (2012). Metabolite profiling identifies a key role for glycine in rapid cancer cell proliferation. *Science* **336**, 1040–1044.
- Jiang, T., Olson, E. S., Nguyen, Q. T., Roy, M., Jennings, P. A. and Tsien, R. Y. (2004). Tumor imaging by means of proteolytic activation of cell-penetrating peptides. *Proc. Natl. Acad. Sci. USA* **101**, 17867–17872.
- Kowalczyk, S., Winkelman, A., Smolinsky, B., Förster, B., Neundorff, I., Schwarz, G. and Meier, J. C. (2013). Direct binding of GABA_A receptor $\beta 2$ and $\beta 3$ subunits to gephyrin. *Eur. J. Neurosci.* **37**, 544–554.
- Kuhse, J., Kuryatov, A., Maulet, Y., Malosio, M. L., Schmieden, V. and Betz, H. (1991). Alternative splicing generates two isoforms of the alpha 2 subunit of the inhibitory glycine receptor. *FEBS Lett.* **283**, 73–77.
- Labrakakis, C., Patt, S., Hartmann, J. and Kettenmann, H. (1998). Functional GABA(A) receptors on human glioma cells. *Eur. J. Neurosci.* **10**, 231–238.
- Laks, D. R., Masterman-Smith, M., Visnyei, K., Angenieux, B., Orozco, N. M., Foran, I., Yong, W. H., Vinters, H. V., Liau, L. M., Lazareff, J. A. et al. (2009). Neurosphere formation is an independent predictor of clinical outcome in malignant glioma. *Stem Cells* **27**, 980–987.
- Legendre, P., Förster, B., Jüttner, R. and Meier, J. C. (2009). Glycine receptors caught between genome and proteome – Functional implications of RNA editing and splicing. *Front. Mol. Neurosci.* **2**, 23.
- Malosio, M. L., Grenningloh, G., Kuhse, J., Schmieden, V., Schmitt, B., Prior, P. and Betz, H. (1991). Alternative splicing generates two variants of the alpha 1 subunit of the inhibitory glycine receptor. *J. Biol. Chem.* **266**, 2048–2053.
- Meier, J. and Grantyn, R. (2004). Preferential accumulation of GABA(A) receptor $\gamma 2L$, not $\gamma 2S$, cytoplasmic loops at rat spinal cord inhibitory synapses. *J. Physiol.* **559**, 355–365.
- Meier, J., Vannier, C., Sergé, A., Triller, A. and Choquet, D. (2001). Fast and reversible trapping of surface glycine receptors by gephyrin. *Nat. Neurosci.* **4**, 253–260.
- Meier, J., Jüttner, R., Kirischuk, S. and Grantyn, R. (2002). Synaptic anchoring of glycine receptors in developing collicular neurons under control of metabotropic glutamate receptor activity. *Mol. Cell. Neurosci.* **21**, 324–340.
- Melzer, N., Villmann, C., Becker, K., Harvey, K., Harvey, R. J., Vogel, N., Kluck, C. J., Kneussel, M. and Becker, C. M. (2010). Multifunctional basic motif in the glycine receptor intracellular domain induces subunit-specific sorting. *J. Biol. Chem.* **285**, 3730–3739.
- Meyer, G., Kirsch, J., Betz, H. and Langosch, D. (1995). Identification of a gephyrin binding motif on the glycine receptor beta subunit. *Neuron* **15**, 563–572.
- Nanba, D., Mammoto, A., Hashimoto, K. and Higashiyama, S. (2003). Proteolytic release of the carboxy-terminal fragment of proHB-EGF causes nuclear export of PLZF. *J. Cell Biol.* **163**, 489–502.
- Nikolic, Z., Laube, B., Weber, R. G., Lichter, P., Kioschis, P., Poustka, A., Mühlhardt, C. and Becker, C. M. (1998). The human glycine receptor subunit alpha3. Glra3 gene structure, chromosomal localization, and functional characterization of alternative transcripts. *J. Biol. Chem.* **273**, 19708–19714.
- Notelaers, K., Smisdom, N., Rocha, S., Janssen, D., Meier, J. C., Rigo, J. M., Hofkens, J. and Ameloot, M. (2012). Ensemble and single particle fluorimetric techniques in concerted action to study the diffusion and aggregation of the glycine receptor $\alpha 3$ isoforms in the cell plasma membrane. *Biochim. Biophys. Acta* **1818**, 3131–3140.
- Silvestre, D. C., Pineda, J. R., Hoffschir, F., Studler, J. M., Mouthon, M. A., Pflumio, F., Junier, M. P., Chneiweiss, H. and Boussin, F. D. (2011). Alternative lengthening of telomeres in human glioma stem cells. *Stem Cells* **29**, 440–451.
- Simon, J., Wakimoto, H., Fujita, N., Lalande, M. and Barnard, E. A. (2004). Analysis of the set of GABA(A) receptor genes in the human genome. *J. Biol. Chem.* **279**, 41422–41435.
- Tasneem, A., Iyer, L. M., Jakobsson, E. and Aravind, L. (2004). Identification of the prokaryotic ligand-gated ion channels and their implications for the mechanisms and origins of animal Cys-loop ion channels. *Genome Biol.* **6**, R4.
- Thirant, C., Bessette, B., Varlet, P., Puget, S., Cadusseau, J., Tavares, S. R., Studler, J. M., Silvestre, D. C., Susini, A., Villa, C. et al. (2011). Clinical relevance of tumor cells with stem-like properties in pediatric brain tumors. *PLoS ONE* **6**, e16375.
- Walzlein, J. H., Synowitz, M., Engels, B., Markovic, D. S., Gabrusiewicz, K., Nikolaev, E., Yoshikawa, K., Kaminska, B., Kempermann, G., Uckert, W. et al. (2008). The antitumorigenic response of neural precursors depends on subventricular proliferation and age. *Stem Cells* **26**, 2945–2954.
- Winkelmann, A., Maggio, N., Eller, J., Caliskan, G., Semtner, M., Häussler, U., Jüttner, R., Dugladze, T., Smolinsky, B., Kowalczyk, S. et al. (2014). Changes in neural network homeostasis trigger neuropsychiatric symptoms. *J. Clin. Invest.* **124**, 696–711.
- Zuleger, N., Kerr, A. R. and Schirmer, E. C. (2012). Many mechanisms, one entrance: membrane protein translocation into the nucleus. *Cell. Mol. Life Sci.* **69**, 2205–2216.